1768 *Inorg. Chem.* **1988**, *27*, 1768–1775

Contribution from the Department of Chemistry, D-006,
University of California at San Diego, La Jolla, California 92093

Kinetics of Cis–Trans Isomerization and Reductive Elimination in Dihydridobis(trimethylphosphine)platinum(II)

Diane L. Packett and William C. Trogler*

Received January 28, 1988

Solutions of $PtH_2(PMe_3)_2$ (**1**) exist as an equilibrium mixture of cis and trans isomers, with the cis isomer dominating in polar solvents. The forward rate constant for trans $\leftrightarrow$ cis isomerization was determined by spin-saturation-transfer studies to be ~0.1 s^{-1} at −60 °C. The isomerization may proceed by an associative mechanism involving a phosphine ligand or solvent molecule, or by dissociation of PMe_3 from the cis and trans isomers to form T-shaped intermediates that slowly interconvert. Above −35 °C the phosphine ligands exchange rapidly between the isomers of **1** with rate constants in the range 7–600 s^{-1}. Addition of a trace of free phosphine to solutions of **1** results in the formation of $PtH_2(PMe_3)_3$ (**2**), which exchanges phosphine ligands rapidly with *trans*-**1** but not with *cis*-**1**. Under a nitrogen atmosphere, **1** decomposes by unimolecular rate-determining reductive elimination of hydrogen with an inverse kinetic isotope effect, $k_H/k_D = 0.45 \pm 0.1$. This inversion isotope effect supports the theoretical predictions of nearly complete H–H bond formation in the transition state for reductive elimination. In coordinating THF solvent, reductive elimination of H_2 occurs slowly, with $\Delta H^{\ddagger} = 9.4 \pm 1$ kcal mol^{-1} and $\Delta S^{\ddagger} = -41 \pm 3$ cal mol^{-1} deg^{-1}. The large negative entropy of activation reflects solvent reorganization in the transition state. In noncoordinating Me_4THF solvent elimination of hydrogen proceeds more rapidly, with $\Delta H^{\ddagger} = 20.0 \pm 0.5$ kcal mol^{-1} and $\Delta S^{\ddagger} = -1 \pm 2$ cal mol^{-1} deg^{-1}. This value of $\Delta H^{\ddagger}$, as well as the large inverse isotope effect, compares favorably with theoretical calculations for hydrogen elimination from **1** and yields an estimate for the Pt–H bond dissociation energy of 62 kcal mol^{-1}.

Introduction

Dihydridobis(phosphine)platinum(II) complexes have been studied as possible intermediates in homogeneous hydrogenation catalysis[1] and as models for the behavior of hydrogen on a platinum surface. Much is known about the reactivity of platinum dihydrides containing bulky phosphine ligands.[2] In recent years sterically unhindered dihydrides PtH_2L_2 (L = PEt_3, PMe_3) have been isolated and found[3-7] to be much more reactive than analogues containing bulky phosphine ligands.

The activation of molecular hydrogen is an important process in homogeneous and heterogeneous catalytic reactions.[8-12] Although mechanistic studies of the reductive elimination of C–H[13-16] and C–C[17-21] bonds from metal complexes have been reported, less is known about the intramolecular reductive elimination of hydrogen from mononuclear metal complexes. Intermolecular reductive elimination of H_2 from metal clusters has been suggested as a model for the behavior of hydrogen on metal surfaces.[22] Sterically unhindered platinum dihydrides have been investigated in several theoretical studies,[23-26] which focus on the reductive elimination of hydrogen from the platinum center. This elimination has been suggested to proceed through a "late" transition state that resembles the reaction products, or perhaps contains an η^2-hydrogen ligand. Predicted barriers[23-26] for reductive elimination of H_2 from *cis*-PtH_2L_2 (L = PH_3 or PMe_3) range between 18 and 42 kcal/mol. The isolation of the sterically unhindered dihydride *trans*-$PtH_2(PMe_3)_2$ permits direct observation of cis–trans isomerization and intramolecular reductive elimination of hydrogen. We report here experimental investigations of the reaction mechanisms of these fundamental processes to compare with theoretical predictions. A portion of this work has been previously communicated.[6]

Experimental Section

General Procedures. Reactions were carried out by using standard Schlenk techniques under an atmosphere of prepurified nitrogen or hydrogen. Reactions monitored by NMR spectroscopy were contained in NMR tubes sealed with septum caps and flushed with nitrogen. Unless noted, all procedures were carried out at ambient temperature.

---

(1) Yoshida, T.; Yamagata, T.; Tulip, T. H.; Ibers, J. A.; Otsuka, S. *J. Am. Chem. Soc.* **1978**, *100*, 2063–2073.

(2) (a) Leviston, P. G.; Wallbridge, M. G. H. *J. Organomet. Chem.* **1976**, *110*, 271–279. (b) Clark, H. C.; Goel, A. B.; Wong, C. S. *Ibid.* **1978**, *152*, C45–C47. (c) Yoshida, T.; Otsuka, S. *J. Am. Chem. Soc.* **1977**, *99*, 2134–2140. (d) Goel, A. B.; Goel, S. *Inorg. Chim. Acta* **1982**, *65*, L77–L78. (e) Clark, H. C.; Goel, A. B.; Goel, R. G.; Ogini, W. O. *J. Organomet. Chem.* **1978**, *157*, C16–C18. (f) Immirzi, A.; Musco, A.; Carturan, G.; Belluco, U. *Inorg. Chim. Acta* **1975**, *12*, L23–L24. (g) Shaw, B. L. *ACS Symp. Ser.* **1982**, *No. 196*, 101–126. (h) Stone, F. G. A. *Angew. Chem., Int. Ed. Engl.* **1984**, *23*, 89–99. (i) Venanzi, L. M. *Coord. Chem. Rev.* **1982**, *43*, 251–274. (j) Moulton, C. J.; Shaw, B. L. *J. Chem. Soc., Chem. Commun.* **1976**, 365–366. (k) Albinati, A.; Musco, A.; Carturan, G.; Strukul, G. *Inorg. Chim. Acta* **1976**, *18*, 219–223. (l) Immirzi, A.; Musco, A. *Ibid.* **1977**, *22*, L35–L36. (m) Ebsworth, E. A. V.; Marganian, V. M.; Reed, F. J. S.; Gould, R. O. *J. Chem. Soc., Dalton Trans.* **1978**, 1167–1170. (n) Clark, H. C.; Goel, A. B.; Billard, C. *J. Organomet. Chem.* **1979**, *182*, 431–440. (o) Clark, H. C.; Goel, A. B.; Wong, C. S. *Inorg. Chim. Acta* **1979**, *34*, 159–160. (p) Clark, H. C.; Hampden-Smith, M. J. *Coord. Chem. Rev.* **1987**, *79*, 229–255.

(3) (a) Paonessa, R. S.; Trogler, W. C. *J. Am. Chem. Soc.* **1982**, *104*, 1138–1140. (b) Paonessa, R. S.; Prignano, A. L.; Trogler, W. C. *Organometallics* **1985**, *4*, 647–657.

(4) Gerlach, D. H.; Kane, A. R.; Parshall, G. W.; Jesson, J. P.; Muetterties, E. L. *J. Am. Chem. Soc.* **1971**, *93*, 3543–3544.

(5) Packett, D. L.; Jensen, C. M.; Cowan, R. L.; Strouse, C. E.; Trogler, W. C. *Inorg. Chem.* **1985**, *24*, 3578–3583.

(6) Packett, D. L.; Trogler, W. C. *J. Am. Chem. Soc.* **1986**, *108*, 5036–5038.

(7) Packett, D. L.; Syed, A.; Trogler, W. C. *Organometallics* **1988**, *7*, 159–166.

(8) Collman, J. P.; Hegedus, L. S.; Norton, J. R.; Finke, R. *Principles and Applications of Organotransition Metal Chemistry*, 2nd ed.; University Science Books: Mill Valley, CA, 1987; Chapter 5.

(9) Halpern, J. *Acc. Chem. Res.* **1970**, *3*, 386–392.

(10) James, B. R. *Homogeneous Hydrogenation*; Wiley: New York, 1973.

(11) Vaska, L. *Acc. Chem. Res.* **1968**, *1*, 335–344.

(12) Davis, S. C.; Klabunde, K. J. *Chem. Rev.* **1982**, *82*, 153–208.

(13) Abis, L.; Sen, A.; Halpern, J. *J. Am. Chem. Soc.* **1978**, *100*, 2915–2916.

(14) Michelin, R. A.; Faglia, S.; Uguagliati, P. *Inorg. Chem.* **1983**, *22*, 1831–1834.

(15) Buchanan, J. M.; Stryker, J. M.; Bergman, R. G. *J. Am. Chem. Soc.* **1986**, *108*, 1537–1550.

(16) Okrasinski, S. J.; Norton, J. R. *J. Am. Chem. Soc.* **1977**, *99*, 295–297.

(17) Braterman, P. S.; Cross, R. J.; Yong, G. B. *J. Chem. Soc., Dalton Trans.* **1977**, 1892–1897.

(18) Moravskiy, A.; Stille, J. K. *J. Am. Chem. Soc.* **1981**, *103*, 4182–4186.

(19) Gillie, A.; Stille, J. K. *J. Am. Chem. Soc.* **1980**, *102*, 4933–4941.

(20) Norton, J. R. *Acc. Chem. Res.* **1979**, *12*, 139–145.

(21) Tamaki, A.; Magennis, S. A.; Kochi, J. K. *J. Am. Chem. Soc.* **1974**, *96*, 6140–6148.

(22) (a) Bavaro, L. M.; Montangero, P.; Keister, J. B. *J. Am. Chem. Soc.* **1983**, *105*, 4977–4981. (b) Duggan, T. P.; Barnett, D. J.; Muscatella, M. J.; Keister, J. B. *Ibid.* **1986**, *108*, 6076–6077. (c) Lloyd, B. R.; Puddephatt, R. J. *Ibid.* **1985**, *107*, 7785–7786. (d) Dutta, T. K.; Meng, X.; Vites, J. C.; Fehlner, T. P. *Organometallics* **1987**, *6*, 2191–2200.

(23) Noell, J. O.; Hay, P. J. *J. Am. Chem. Soc.* **1982**, *104*, 4578–4584.

(24) (a) Low, J. J.; Goddard, W. A., III. *J. Am. Chem. Soc.* **1984**, *106*, 6928–6937. (b) Low, J. J.; Goddard, W. A., III. *Organometallics* **1986**, *5*, 609–622.

(25) Obara, S.; Kitaura, K.; Morokuma, K. *J. Am. Chem. Soc.* **1984**, *106*, 7482–7492.

(26) Balazs, A. C.; Johnson, K. H.; Whitesides, G. M. *Inorg. Chem.* **1982**, *21*, 2162–2174.

0020-1669/88/1327-1768$01.50/0

Materials. Hydrogen (99.999%) and deuterium (CP grade) were obtained from Liquid Carbonics. High-purity hydrogen must be used to avoid decomposition side reactions. Tetrahydrofuran (Mallinckrodt) was dried over potassium benzophenone ketyl and distilled under nitrogen. Dimethyl- and tetramethyltetrahydrofuran (Aldrich) were dried over sodium benzophenone ketyl and distilled under nitrogen. *n*-Hexane (Aldrich, 99%) was dried over lithium aluminum hydride and distilled under nitrogen. Dimethyl-d_6 sulfoxide and acetone-d_6 (Aldrich) were dried over 4A molecular sieves and were degassed. Trimethylphosphine (Strem), naphthalene = Nap (Aldrich Gold Label), diethyl sulfide (Aldrich), and THF-d_8 (Cambridge Isotopes) were used as received.

Physical Measurements. Infrared spectra were obtained with an IBM FTIR 32 spectrometer in 0.1-mm path length CaF_2 cells that were flushed with nitrogen, argon, or hydrogen before use. Gas chromatographic separations of H_2:HD:D_2 mixtures were performed with a Hewlett-Packard 5890A instrument using a thermal conductivity detector. The column for separating H_2 and D_2 consisted of a 6-ft $FeCl_3$/alumina column and a 12-in. CuO furnace.[27] The ^{31}P NMR spectra were obtained with a Nicolet 200 spectrometer at 80.99 MHz. Proton NMR spectra were obtained with a General Electric QE 300 spectrometer at 300.15 MHz. All chemical shifts are positive in the direction of increasing frequency. Proton chemical shifts were referenced to the deuteriated solvent resonance. Phosphorus chemical shifts were referenced to the deuterium resonance of the solvent by using the internal frequency lock of the spectrometer such that the resonance of a capillary of 85% H_3PO_4, centered in a 10-mm NMR tube of the deuteriated solvent, appeared at 0 ppm at 20 °C.

Preparation of *trans*-$PtH_2(PMe_3)_2{\cdot}C_{10}H_8$, Pt(H)(D)$(PMe_3)_2$, and *trans*-$PtD_2(PMe_3)_2{\cdot}C_{10}H_8$. The dihydride complex was prepared according to procedures described previously.[5] The dideuteride was prepared by the same method, with the following changes. The volume of a freshly prepared solution of the dihydride was reduced to ~2 mL by rapid purging with hydrogen. Next deuterium was bubbled through the solution for about 5 min. Five milliliters of *n*-hexane were layered on the solution. Cooling to −40 °C for 16 h under D_2 produced white crystals of the dideuteride. Analysis of the gas evolved from PtD_2L_2 by gas chromatography revealed that it contained <5% $PtHDL_2$ impurity.

The Pt(H)(D)$(PMe_3)_2$ complex was generated from the dideuteride, dissolved in acetone-d_6 under a deuterium atmosphere, by bubbling H_2 through the solution for ~1 min and letting the H_2/D_2 exchange process come to equilibrium. The dominant species present was the dideuteride, a small amount of the hydride–deuteride complex, and a smaller amount of dihydride. Thus the proton NMR spectrum (in the hydride region) is that of the hydride–deuteride complex.

Preparation of $PtH_2(PMe_3)(PEt_3)$. Solutions of $PtH_2(PMe_3)_2$ and $PtH_2(PEt_3)_2$ were generated independently from the $PtCl_2L_2$ complexes in THF solution. The solutions were each reduced to ~2 mL with a rapid hydrogen purge and mixed in a 10-mm NMR tube under a H_2 atmosphere. The $^{31}P\ \{^1H\}$ NMR at −40 °C revealed a mixture of $PtH_2(PMe_3)_2$, $PtH_2(PEt_3)_2$, and *trans*-$PtH_2(PEt_3)(PMe_3)$. The resonance for each phosphorus ligand in the latter complex appeared as a doublet, $^2J_{P-P}$ = 411 Hz, centered about the resonance for the corresponding bis(phosphine) dihydride at +28.5 and −20.5 ppm, with $^1J_{Pt-P}$ = 2700 Hz. Only the trans isomer of the mixed-phosphine complex was detected.

IR Kinetic Studies of H_2 Reductive Elimination. Isolated *trans*-$PtH_2L_2{\cdot}C_{10}H_8$ was dissolved in the desired solvent to a known concentration under a H_2 atmosphere. Reactions were carried out by admitting an N_2 atmosphere in Schlenk tubes placed in a thermostated bath. At timed intervals, aliquots were withdrawn by syringe and transferred into 0.1-mm CaF_2 liquid-sample cells. The nitrogen atmosphere was exchanged frequently to prevent the buildup of hydrogen, which can back-react and slow the reductive elimination reaction. The reaction was followed by monitoring the decrease in the absorbances at 1980 or 1720 cm^{-1}. The absorbances that were monitored obeyed Beer's law over the concentration range of interest. For measurements below 20 °C, the IR cells were precooled by purging with nitrogen that was passed through a copper coil in an N_2/pentane slush bath at −130 °C. Infinity points for the reaction were determined by the Kezdy–Swinbourne method.[28]

Isotope Effect on Reductive Elimination and H_2/D_2 Exchange. To determine the kinetic isotope effect for the reductive elimination, as well as detect isotopic exchange, $PtH_2L_2{\cdot}$Nap and $PtD_2L_2{\cdot}$Nap were allowed to decompose together in THF solvent. The isotopomers were synthesized and isolated independently and weighed in Schlenk tubes under an atmosphere of hydrogen or deuterium. The solid samples were cooled to −78 °C and quickly transferred into a flask under a nitrogen atmosphere. About 3 mL of dry, degassed THF was added, and the mixture was warmed to room temperature. The solid PtH_2L_2 and PtD_2L_2 dissolved and began to decompose. The atmosphere over the solution was sampled at intervals and analyzed by gas chromatography[27] to give the isotope effect from the H_2:D_2 product ratio. At short reaction times H_2/D_2 exchange to HD does not appreciably affect these measurements.

Spin-Saturation-Transfer Studies of the Rate of Cis–Trans Isomerization. Isolated *trans*-$PtH_2L_2{\cdot}$Nap was dissolved in the desired solvent in a 5-mm NMR tube under a hydrogen atmosphere. The NMR probe was cooled to the appropriate temperature and retuned. The sample was allowed to come to thermal equilibrium in the probe for 15 min. The ^1H NMR spectra obtained were referenced to the solvent resonance. Apparent spin–lattice relaxation times for *cis*- and *trans*-**1** were determined by the inversion-recovery method while the exchanging resonance was saturated. A radio frequency pulse was applied at the center of the multiplet, with the minimum decoupler power necessary to saturate the resonance used. The inversion-recovery pulse sequence was modified to allow decoupling during delays but not during acquisitions. Saturation-transfer studies[29–31] were carried out by acquiring the spectrum while one of the exchanging resonances was being saturated. The spectrum was also acquired while irradiation on the opposite side (up- or downfield) of the observed peak took place, at a distance equal to the chemical shift difference between the resonances of *cis*- and *trans*-**1**. This determined the equilibrium intensity of the peak observed, corrected for the spillover of decoupler power.[31] This was a concern in these experiments because of the small frequency difference between *cis*- and *trans*-**1**. Measurements were repeated five times and averaged.

Spectral Simulations of the Phosphine-Exchange Process. To approximate the rate constants for self-exchange to phosphine ligands in *cis*- and *trans*-**1**, the proton NMR spectra at temperatures between −35 and +25 °C were simulated[32] by using a computer program developed by Perrin and Johnston.[33] NMR line shapes were calculated from the equation

$$I(\omega) \propto \mathrm{Im}\{i\mathbf{1} - \mathbf{T}_2[\mathbf{T}_2 + i\mathbf{X} - i\mathbf{\Omega} + \mathbf{K}]^{-1}\mathbf{p}\} = \mathrm{Im}\{i\mathbf{1}\mathbf{S}^{-1}[\mathbf{D} + i\mathbf{X}]^{-1}\mathbf{S}\mathbf{p}\}$$

where **1** is a unit-row matrix, $\mathbf{T}_2 = \mathrm{diag}(1/T_{2i}) = \mathrm{diag}(\pi\delta\nu_i^0)$, $\mathbf{\Omega} = \mathrm{diag}(\omega_i)$, $\mathbf{K}_{ij} = k_{ji}\ (i \neq j)$, $K_{ii} = -\Sigma_j k_{ij}$, $\mathbf{X} = \mathrm{diag}(\omega)$, **p** is a column matrix of populations, and **S** is the transformation matrix that diagonalizes $\mathbf{T}_2 - i\mathbf{\Omega} + \mathbf{K}$ to $\mathbf{D} = \mathbf{S}(\mathbf{T}_2 - i\mathbf{\Omega} + \mathbf{K})\mathbf{S}^{-1}$.[33] Input parameters are site populations, chemical shifts in Hz, T_2 values in the absence of exchange [related to the width at half-height for each signal by $T_2 = 1/(\pi\Delta\nu^0{}_{1/2})$], and first-order rate constants for site interchange.[33] The seven lines of the central triplet (*trans*-**1**) and doublet of doublets (*cis*-**1**) were simulated as eight sites. The 1:2:1 triplet resonance of *trans*-**1** was simulated as a 1:1:1:1 quartet with the central peaks having the same chemical shift. Resonances from the ^{195}Pt satellites were not simulated. The peaks of the 1:1:1:1 quartet of the trans isomer were designated as sites 1–4. To simulate exchange of PMe_3 from *trans*-**1**, rate constants for self-exchange were input as $k_{1,2}$, $k_{1,3}$, $k_{2,3}$, $k_{2,4}$, and $k_{3,4}$; since only one rate constant was involved, these values were all equal. The peaks of the quartet resonance of *cis*-**1** were designated as sites 5–8, with the rate constants $k_{5,6}$, $k_{5,7}$, $k_{6,7}$, $k_{6,8}$, and $k_{7,8}$ being input. The input values of the rate constants were adjusted until the simulated spectra visually matched the experimental spectra.

Results

Physical Properties and Solution Structure of 1. *trans*-$PtH_2(PMe_3)_2{\cdot}C_{10}H_8$ (**1**) is synthesized by reduction of *cis*-$PtCl_2(PMe_3)_2$ with 2 equiv of sodium naphthalide under a hydrogen atmosphere.[5] It crystallizes from THF/*n*-hexane as an inclusion complex of naphthalene. Although the trans isomer crystallizes, in solution **1** exists as an equilibrium mixture of cis and trans isomers, and the polar cis isomer dominates in polar solvents. The ^1H NMR spectrum of **1** (Figure 1), shows the triplet pattern expected for the trans isomer, with ^{195}Pt satellites (J_{Pt-H} = 807 Hz), centered at δ −2.7. A more complex second-order doublet of doublet resonance for the cis isomer appears upfield, centered at δ −3.7, about a ^{195}Pt satellite of the trans isomer. Equilibrium studies have shown that the energy difference between isomers is within

---

[27] Shipman, G. F. *Anal. Chem.* **1962**, *34*, 877–878.

[28] Espenson, J. H. *Chemical Kinetics and Reaction Mechanisms*; McGraw-Hill: New York, 1981.

[29] (a) Forsen, S.; Hoffmann, R. *Acta. Chem. Scand.* **1963**, *17*, 1787–1788. (b) Forsen, S.; Hoffmann, R. *J. Chem. Phys.* **1964**, *40*, 1189–1196.

[30] Mann, B. E. *J. Magn. Reson.* **1977**, *25*, 91–94.

[31] Perrin, C. L.; Johnston, E. R. *J. Magn. Reson.* **1979**, *33*, 619–626.

[32] Reeves, L. W.; Shaw, K. N. *Can. J. Chem.* **1970**, *48*, 3641–3653.

[33] (a) Johnston, E. R. Ph.D. Thesis, University of California at San Diego, 1980. (b) Perrin, C. L.; Johnston, E. R.; Lollo, C. P.; Kobrin, P. A. *J. Am. Chem. Soc.* **1981**, *103*, 4691–4696.

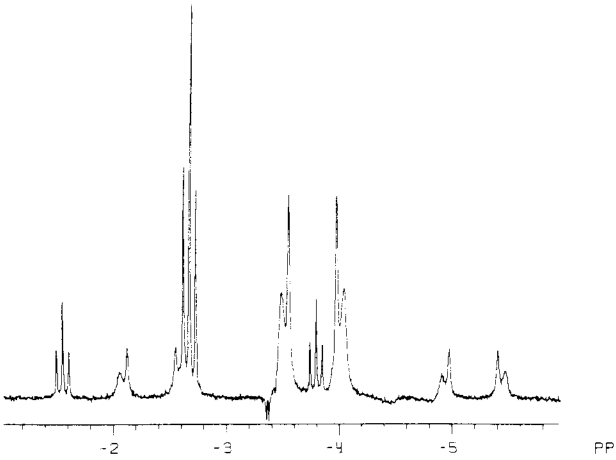

Figure 1. Hydride region of ^{1}H NMR spectrum of $PtH_2(PMe_3)_2$ in acetone-d_6 solvent at -80 °C.

Table I. Apparent T_1 values for PtH_2L_2[a]

T, °C	T_1(*cis*-**1**), s	T_1(*trans*-**1**), s
-50	1.7	4.3
-60	0.5	1.9
-70	1.0	4.1

[a] Acetone-d_6 solvent.

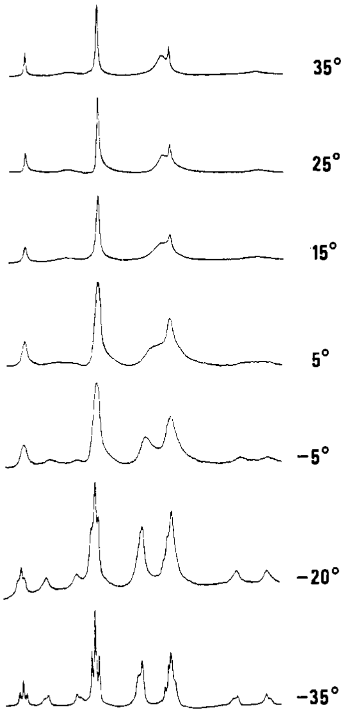

Figure 2. Exchange of phosphine ligand from *cis*- and *trans*-**1**, in THF-d_8 solvent between -35 and +35 °C.

1 kcal/mol in both acetone and toluene solvents.[5] Values of ΔH_{isom} in THF and in 2,5-Me_2THF of 0.57 ± 0.50 and 1.0 ± 0.5 kcal/mol, respectively, show that the coordinating ability of solvent has little effect on the relative stabilities of cis and trans isomers.

We considered the possibility that *cis*-PtH_2L_2 might exist as an η^2-dihydrogen complex. Many such complexes have now been reported,[34-39] including a suggestion of η^2-dihydrogen coordination in *cis*-$PtH_2[Cy_2P(CH_2)_nPCy_2]$,[39] where n = 2, 3, 4. A recent theoretical study[40] concludes that dihydride formation is favored by the presence of electron-donating phosphine ligands on the metal while the π-acid CO ligand favors an η^2-dihydrogen species. The IR spectral data for **1** confirm that *cis*-PtH_2L_2 exists predominantly as a dihydride complex. The symmetric and asymmetric cis Pt-H stretches appear as overlapping bands at 2030 and 1980 cm^{-1}, and the asymmetric stretch of the trans isomer appears at 1720 cm^{-1} in the solution infrared spectrum. An η^2-dihydrogen absorbance typically occurs between 2300 and 2700 cm^{-1}.[34] The absence of the characteristic ~30 Hz H-D coupling in the proton NMR spectrum of $Pt(H)(D)L_2$ also rules against an η^2-HD ligand.

Trans ↔ Cis Isomerization. Structural isomerization of **1** reaches equilibrium when *trans*-**1** is dissolved in acetone-d_6 at -80 °C and placed in the NMR probe at -80 °C (within 20 min).[5] To measure the rate of trans ↔ cis isomerization, spin-saturation-transfer studies[29] were performed. For a two-site exchange process, the intensity I of magnetization at site A is measured in

$$A \underset{k_B}{\overset{k_A}{\rightleftharpoons}} B$$

the presence (I^A) and the absence (I_0^A) of a saturating radio frequency field at B. The negative enhancement at A is given by $(I_0^A - I^A)/I_0^A$, an expression similar to that for nuclear Overhauser enhancement.[30,31] If the spin-lattice relaxation time, T_1, for A is known, then the rate constant k_A can be calculated. If the values of T_1 for A and B are not equal, the T_1's determined by the normal 180°-τ-90° sequence will be averaged over both sites by exchange. Thus, T_{1A} can be measured by the inversion-recovery method while site B is saturated. Mann[30] has shown that this "apparent" T_1 is related to the "true" T_1 value by

$$T_{1A}(\text{app}) = \frac{T_{1A}}{1 + k_A T_{1A}} \tag{1}$$

If this apparent T_1 is determined, the rate constant may be calculated from[30]

$$k_A = \frac{1}{T_{1A}(\text{app})}\left(\frac{I_0^A - I^A}{I_0^A}\right) \tag{2}$$

Table I contains the apparent values of T_1 for *cis*- and *trans*-**1**, measured while the exchanging resonance was being saturated. Relaxation times for both isomers appear to pass through a minimum near -60 °C. At the temperature where a T_1 minimum occurs, the molecular tumbling frequency approximates the nuclear precession (Larmor) frequency, and relaxation occurs most efficiently.[41,42]

The T_1's for both *cis*- and *trans*-**1** are on the order of seconds, which further suggests that *cis*-**1** exists as a dihydride rather than as an η^2-H_2 complex. Because the dominant mechanism for relaxation in η^2-H_2 complexes is the H-H dipolar interaction, and because $1/T_1$ varies as r^{-6}, the short H-H distance results in T_1 values in the range 10-100 ms, near that of molecular hydrogen.[34,36] Crabtree has determined that the T_1's of phosphine-substituted classical metal dihydride complexes range from 0.35 to > 2 s.[35,36] According to eq 1, the apparent T_1 value of 4.3 s and the rate constant for isomerization (vide infra) yield an in-

---

(34) (a) Kubas, G. J.; Ryan, R. R.; Swanson, B. I.; Vergamini, P. J.; Wasserman, H. J. *J. Am. Chem. Soc.* **1981**, *106*, 451-452. (b) Kubas, G. J.; Ryan, R. R.; Wrobleski, D. A. *Ibid.* **1986**, *108*, 1339-1341. (c) Wasserman, H. J.; Kubas, G. J.; Ryan, R. R. *Ibid.* **1986**, *108*, 2294-2301. (d) Kubas, G. J.; Unkefer, C. J.; Swanson, B. I.; Fukushima, E. *Ibid.* **1986**, *108*, 7000-7009. (e) Zilm, K. W.; Merrill, R. A.; Kummer, M. W.; Kubas, G. J. *Ibid.* **1986**, *108*, 7837-7839.

(35) Crabtree, R. H.; Lavin, M. *J. Chem. Soc., Chem. Commun.* **1985**, 1661-1662.

(36) Crabtree, R. H.; Lavin, M.; Bonneviot, L. *J. Am. Chem. Soc.* **1986**, *108*, 4032-4037. For a caveat see: Ammann, C.; Isaia, F.; Pregosin, P. S. *Magn. Reson. Chem.* **1988**, *26*, 236-238.

(37) Sweany, R. L. *J. Am. Chem. Soc.* **1985**, *107*, 2374-2379.

(38) Morris, R. H.; Sawyer, J. F.; Shiralian, M.; Zubkowski, J. D. *J. Am. Chem. Soc.* **1985**, *107*, 5581-5582.

(39) Clark, H. C.; Smith, M. J. H. *J. Am. Chem. Soc.* **1986**, *108*, 3829-3830.

(40) Hay, P. J. *J. Am. Chem. Soc.* **1987**, *109*, 705-710.

(41) (a) Johnson, C. S.; Moreland, C. G. *J. Chem. Educ.* **1973**, *50*, 477-483. (b) Sandstrom, J. *Dynamic NMR Spectroscopy*; Academic: London, 1982.

(42) Becker, E. D. *High Resolution NMR*; Academic: New York, 1980.

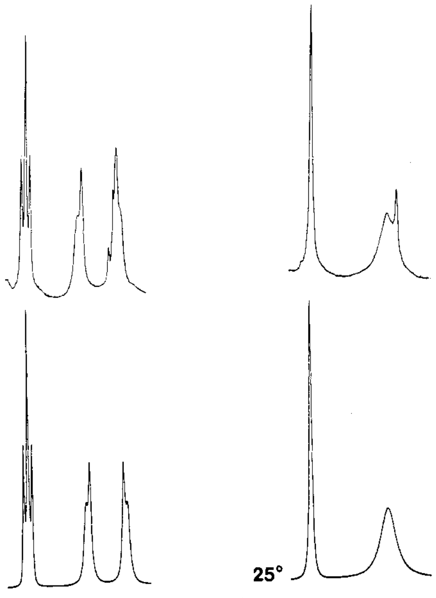

Figure 3. Spectral simulations (bottom) of phosphine exchange spectra (top) from *cis*- and *trans*-**1**, at −35 °C and 25 °C. Exchange rates are given in Table II.

trinsic T_1 of 7.5 s for *trans*-**1** at −50 °C. A measurement of T_1(trans) without saturation of the exchanging cis isomer shows that, at −40 °C, the value of T_1 exceeds 10 s. The intrinsic spin–lattice relaxation times for *cis*- and *trans*-**1** are among the longest known for classical metal hydrides.

Spin-saturation-transfer measurements yield a rate constant for isomerization $k_{\text{trans}\rightarrow\text{cis}} = 0.079\ \text{s}^{-1}$ at −60 °C in acetone-d_6 and a reverse rate constant $k_{\text{cis}\rightarrow\text{trans}} = 0.027\ \text{s}^{-1}$. The ratio of these rate constants gives an equilibrium constant $K = 2.9$ in good agreement with the experimentally determined value of K at −60 °C of 2.8.[5] Because of the small chemical shift difference (1.1 ppm at 300 MHz) between *cis*- and *trans*-**1** and because of the large coupling between the hydride and phosphorus nuclei (Figure 1), the decoupler power necessary to saturate one resonance significantly perturbs the other. This makes it impractical to obtain rates precise enough for measuring an activation barrier. The resonances for *cis*- and *trans*-**1** in the ^{1}H NMR spectrum do not coalesce, even at 35 °C (vide infra). Peak separations require that the rate constant for isomerization should exceed 300 s^{-1} for coalescence to occur, much faster than the rates observed by spin-saturation transfer.[41]

Dissociation of Phosphine Ligands and Formation of $PtH_2(PMe_3)_3$. A solution of *cis*- and *trans*-**1** in THF-d_8 exhibits another dynamic process in the ^{1}H NMR spectrum (Figure 2) at higher temperatures. Between −35 and +5 °C phosphorus–hydrogen coupling gradually disappears, although platinum–hydrogen coupling is retained. Above 5 °C the resonances begin to sharpen into singlets. The Pt–H coupling constants, however, are retained over the entire temperature range −35 to +35 °C. The singlet resonances for *cis*- and *trans*-**1** at 35 °C exhibit platinum satellites with $^1J_{\text{Pt-H}} = 1030$ and 807 Hz, respectively, which lie within 2 Hz of the low-temperature values. These observations suggest that rapid exchange of phosphine ligands occurs between platinum centers but that the Pt–H bond remains intact. The rates of exchange of phosphine ligand from each isomer were determined by spectral simulation (Figure 3). Approximate rate data for the exchange appear in Table II. The same behavior, with similar rate constants, was observed in toluene-d_8 solvent. When $PtH_2(PMe_3)_2$ and $PtH_2(PEt_3)_2$ are mixed at 20 °C, the ^{31}P NMR spectrum of the solution at −40 °C reveals an equilibrium mixture of $PtH_2(PMe_3)_2$, $PtH_2(PEt_3)_2$, and $PtH_2(PMe_3)(PEt_3)$; $^2J_{\text{P-P}} = 400$ Hz. The phosphorus NMR spectra of *cis*- and *trans*-**1** are not resolved above −35 °C because of exchange broadening.

Addition of 1 equiv of PMe_3 to a THF solution of **1** at low temperatures (ca. −70 °C) produces the known five-coordinate species $PtH_2(PMe_3)_3$ (**2**).[3,4] At higher temperatures this compound reductively eliminates hydrogen. If a trace of PMe_3 is added to a solution of **1** at −70 °C, the hydride resonance for the five-coordinate species, **2**, appears at δ −12.8, $^1J_{\text{Pt-H}} = 635$ Hz (Figure 4a). The quartet resonance expected for this complex appears as an exchange-broadened singlet. The resonance for *cis*-**1** also broadens significantly, while the resonance for *trans*-**1** remains well-resolved. This might imply that phosphine ligands exchange rapidly between *cis*-**1** and **2**, but not between *trans*-**1** and **2**. However, saturation of the resonance for **2** markedly decreases the intensity of the resonance for *trans*-**1**, while the broad resonance of *cis*-**1** remains unaffected (Figure 4b). This shows that in fact *trans*-**1** and **2** are rapidly exchanging. This is expected, since the hydride ligands of **2** are trans to each other and this geometry is most easily reached by adding PMe_3 to *trans*-**1**. The broadening of the resonances for *cis*-**1** and **2** suggests that these species also undergo another phosphine ligand exchange process, probably with free PMe_3. Warming this solution to −35 °C shows exchange of phosphine ligands between *cis*- and *trans*-**1**, but **2** is not observed; at these temperatures $Pt(PMe_3)_4$ also begins to form by reductive elimination of hydrogen from **2**. Addition of 1.0 equiv of PMe_3 to this solution results in quantitative formation of $Pt(PMe_3)_4$. Spin-saturation-transfer studies for a sample in

Table II. Rate Data for Exchange of PMe_3 from *cis*- and *trans*-**1** in Acetone-d_6

T, °C	k(*trans*-**1**), s^{-1}	k(*cis*-**1**), s^{-1}
−35	7	7
−20	15	25
−5	30	90
5	40	220
15	60	450
25	125	600
$\Delta H^{\ddagger}$,[a] kcal/mol	5.9 ± 1	10.4 ± 1
$\Delta S^{\ddagger}$, cal/(mol K)	−30 ± 3	−10 ± 2

[a] Because dynamic NMR data depend on spectral line broadening and resolution, the activation parameters obtained are approximate.

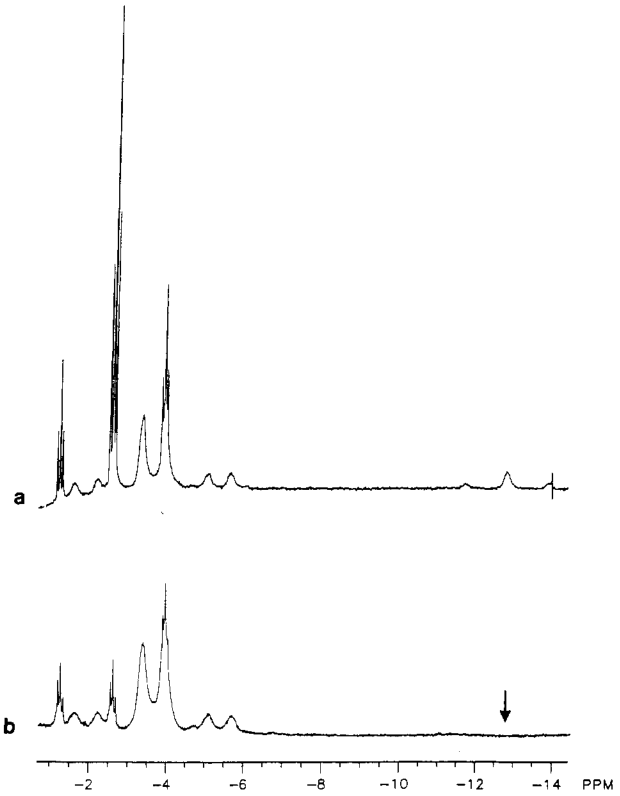

Figure 4. (a) ^{1}H NMR spectrum of *cis*- and *trans*-**1** containing ~1.0% added PMe_3, in THF-d_8 at −70 °C. Peak at −12.8 ppm arises from $PtH_2(PMe_3)_3$ (**2**). (b) ^{1}H NMR spectrum of *cis*- and *trans*-**1** with saturation of the resonance for **2** causing a decrease in intensity of the resonance for *trans*-**1**.

Table III. Kinetic Data for Reductive Elimination of H_2 from Dihydridobis(trimethylphosphine)platinum(II)

	solvent			
	DMSO	THF	2,5-Me_2THF	2,2,5,5-Me_4THF
k,[a] s^{-1}	$5.8 \pm 0.4 \times 10^{-5}$ [b]	$4.4 \pm 0.4 \times 10^{-4}$	$1.1 \pm 0.06 \times 10^{-3}$	$1.79 \pm 0.01 \times 10^{-3}$
$t_{1/2}$, s	11950	1580	630	388
$\Delta H^{\ddagger}$,[c] kcal/mol	10.2 ± 0.5	9.7 ± 1	14.4 ± 0.6	20.5 ± 0.5
$\Delta S^{\ddagger}$,[c] cal/(mol K)	-46 ± 2	-41 ± 3	-23 ± 2	-1 ± 2
log A[d]	3.0	4.3	8.1	12.9

[a] T = 21 °C in THF solvents, 40 °C in DMSO. [b] All errors represent the standard deviation obtained from a linear least-squares analysis. [c] From an Eyring plot. [d] Preexponential factor from an Arrhenius plot.

which the resonances for *cis*-**1** were broadened by exchange, showed no effect on the rate constant k_f for trans → cis isomerization. Thus phosphine ligand exchange and trans → cis isomerization appear to proceed by independent pathways.

That *trans*-**1** and **2** exchange rapidly at −70 °C is evident in the decrease in intensity of the resonance for *trans*-**1** as **2** is irradiated. The broadening of the resonances for *cis*-**1** and **2** must result from exchange with the traces of free PMe_3 introduced into the solution. The five-coordinate complex **2** exchanges with both PMe_3 and *trans*-**1** as in eq 3. A five-coordinate complex is also

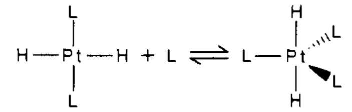

(3)

a possible intermediate for the reaction between *cis*-**1** and PMe_3 (eq 4). The five-coordinate complex formed from *cis*-**1** would

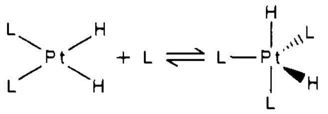

(4)

contain an axial phosphine ligand labilized by trans hydride; consequently, the lifetime of this species might be so short that it would not exist in sufficient concentration to be observed in the ^1H NMR spectrum. It is evident that the exchange process that causes the broadening of *cis*-**1** in Figure 4 is not dissociative, as this exchange is only observed in the presence of excess PMe_3 at these low temperatures (−70 °C). Furthermore, the addition of slightly greater amounts of PMe_3 increases the broadening of the resonances for both **1** and **2**. Thus the exchange process probably involves association of PMe_3 to *cis*-**1**.

Reductive Elimination of Hydrogen. When a solution of *cis*- and *trans*-**1** is exposed to nitrogen, it evolves H_2 to ultimately yield PtL_4 and platinum metal (eq 5).

$$trans\text{-}PtH_2(PMe_3)_2 \underset{K}{\overset{\text{fast}}{\rightleftharpoons}} cis\text{-}PtH_2(PMe_3)_2 \xrightarrow{k_1} Pt(PMe_3)_4 + Pt_x + H_2 \quad (5)$$

Decomposition produces an orange solution with PtL_4 as the major product observed by ^{31}P NMR spectroscopy. The orange color may arise from the presence of phosphidoplatinum clusters; however, no other signals were detected in the ^{31}P NMR spectrum. On standing, this solution produces an insoluble and unstable orange precipitate, presumably consisting of PtL_4 and unidentified cluster complexes formed from PtL_2. Similar products were observed in a study of alkane elimination from $Pt(H)(C_2F_5)(PEt_3)_2$.[14] It was not possible to trap the intermediate PtL_2 species by reaction with an olefin or acetylene since **1** reacts rapidly with such substrates by an associative pathway.[7]

Decomposition of **1** was followed by monitoring the decrease in the IR absorbances of *cis*- or *trans*-**1** at temperatures above −10 °C.[43] Decay of the absorbances for both isomers proceeds at the same rate, which confirms that trans ↔ cis isomerization occurs much faster than reductive elimination (vide supra). Compound **1** decays according to a first-order rate law k_{obsd}-$[PtH_2(PMe_3)_2]$, and we propose the mechanism of eq 5, $k_{obsd} = k_1(K/(K + 1))$. First-order plots for the disappearance of **1** were linear for several half-lives of the reaction. The rate constant k_1 was unaffected by the initial concentration of **1** (0.1–0.3 M)[44] or by the presence of colloidal platinum in the solution. Rates were the same regardless whether **1** was generated in situ in a THF solution or crystallized and redissolved in THF to a known concentration. Rates were the same (±15%) under nitrogen and argon, precluding the formation of a N_2 adduct as an intermediate in the reaction. Rate data and activation parameters are given in Table III.

Comparison of the rate of decomposition of $PtD_2(PMe_3)_2$ in THF at 21 °C with that of $PtH_2(PMe_3)_2$ showed an inverse kinetic isotope effect, reported previously as 0.72 ± 0.06.[6] This value resulted from measurement of the rate of decomposition of PtD_2L_2, by following the decrease in absorbance of a phosphorus–carbon stretch at 1280 cm^{-1}. Interference by an overlapping absorbance made estimation of peak heights difficult and probably introduces a systematic error. Recalculation of k_D based on monitoring of the Pt–D stretch at 1235 cm^{-1} gives an isotope effect of 0.45 ± 0.10 (standard deviation for three determinations). To further test the measurement, a competition experiment was carried out. Equal amounts of PtH_2L_2 and PtD_2L_2 were allowed to decompose together in THF solvent, and the evolved gases were analyzed by gas chromatography near the beginning of the reaction. Ratios of evolved H_2 and D_2 yield an isotope effect of $k_H/k_D = 0.39$. Thus, the inverse isotope effect (0.4–0.45) is even greater than we previously believed. This difference is qualitatively evident in the stability of PtD_2L_2, which decomposes in THF much more rapidly than PtH_2L_2 under the same conditions. Even under an atmosphere of D_2, crystals or solutions of the sensitive dideuteride are best handled at subambient temperatures to avoid decomposition.

These experiments also eliminate the possibility of a mechanism involving dinuclear reductive elimination.[20,45] Although PtH_2L_2 species catalyze H_2/D_2 exchange to HD,[3] the crossover experiments at low conversions were possible because H_2/D_2 exchange is slow relative to reductive elimination. The evolved gas showed only H_2 and D_2 (<5% HD present), which suggests that reductive elimination occurs by an intramolecular process.

We could not investigate the effect of an equivalent of added PMe_3 on the rate of reductive elimination, because free phosphines react with **1** to generate $PtH_2(PMe_3)_3$ (**2**) and ultimately $Pt(PMe_3)_4$ (vide supra). However, the inverse isotope effect shows that the rate-determining step must involve Pt–H bond rupture or formation of an η^2-H_2 complex in a preequilibrium step instead of phosphine dissociation. Rate-determining phosphine dissociation was not observed in a related reaction, the reductive elimination of methane from *cis*-$Pt(H)(CH_3)(PPh_3)_2$.[13] Addition of a trace (1%) of PMe_3 to a solution of **1** in THF had no catalytic effect on the rate of reductive elimination.

The rates of reductive elimination and the activation parameters depend strongly on the coordinating ability of solvent (Table III). The reaction proceeds slowest in THF, although the enthalpic barrier to reductive elimination is only 9.4 kcal/mol. The slow rate arises from the large negative entropy of activation. In

---

(43) It was not possible to monitor the reaction by NMR spectroscopy since the resonances for *cis*- and *trans*-**1** are not resolved above −30 °C where the reactions occur.

(44) High concentrations of **1** were necessary to obtain IR absorbances of sufficient intensity for kinetic studies.

(45) Evans, J.; Norton, J. R. *J. Am. Chem. Soc.* **1974**, *96*, 7577–7578.

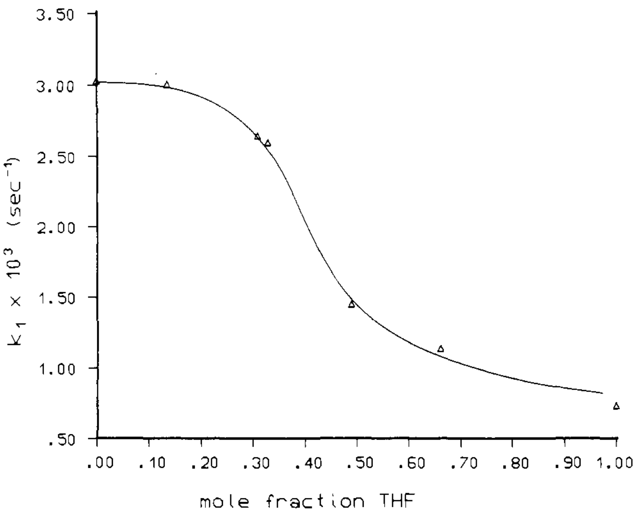

Figure 5. Variation of k_1 with the mole fraction of THF at 21 °C.

2,5-dimethyltetrahydrofuran or in 2,2,5,5-tetramethyltetrahydrofuran solvents, which have dielectric constants nearly identical with that of THF but successively poorer coordinating ability, the enthalpic barrier increases to a maximum of 20.0 kcal/mol, while the entropy decreases to near zero, resulting in a lower $\Delta G^\ddagger$ and faster reaction rate. Rates determined in *n*-hexane solvent [$(2.63 \pm 0.04) \times 10^{-3}$ s^{-1} at 21 °C] resemble those determined in 2,2,5,5-Me_4THF. In DMSO, which has a greater coordinating ability than THF, the reductive elimination only proceeds at high (40–70 °C) temperatures to yield an activation enthalpy of 10.2 ± 0.5 kcal/mol and an activation entropy of -46 ± 2 cal/(mol K). To test for stoichiometric participation of coordinating solvent in the reaction mechanism, the reaction was followed in THF/Me_4THF mixtures. A plot of k_1 vs mole fraction of THF was neither linear nor consistent with a simple rate law (Figure 5). Thus the role of coordinating solvent in the reaction is unclear and appears to be a solvation entropy effect.

Activation of Carbon–Hydrogen Bonds. Intermolecular activation of carbon–hydrogen bonds of alkanes, alkynes, and arenes has been observed for several metal systems.[15,46,47] The reaction may be assisted thermally[46] or photochemically.[47] A recent study of the elimination of neopentane from *cis*-Pt(H)(C_5H_{11})($PCy_2CH_2CH_2PCy_2$) suggests that the generated species Pt($PCy_2CH_2CH_2PCy_2$) activates carbon–hydrogen bonds in a process believed to model the behavior of an "edge" atom on a platinum surface.[48,49] The unsaturated $Pt(PMe_3)_2$ species generated in the reductive elimination of hydrogen from **1** was not observed to add C–H bonds. Photolysis (UV irradiation) or thermolysis of **1** in benzene or hexane under nitrogen resulted in formation of PtL_4 and platinum metal. Presumably ligand rearrangement of $Pt(PMe_3)_2$ occurs faster than the reaction with C–H bonds of solvent.

Discussion

Mechanism of Isomerization and Phosphine Exchange. Possible mechanisms for the isomerization of square-planar complexes have been studied in detail.[50-54] Nonphotochemical isomerization pathways may be divided into three categories: (1) the consecutive displacement mechanism, in which an incoming ligand[50] or solvent[51] molecule displaces an ionic leaving group, usually a halide; (2) pseudorotation of a 5-coordinate species formed by association of a ligand or solvent molecule;[52,53] (3) dissociation of a ligand to form a "T"- or "Y"-shaped intermediate.[54] Most systems studied belong to the class of compounds PtX_2L_2 or $PtRXL_2$ (X = halide; R = alkyl).

A mechanism consistent with our observations is a pseudorotation pathway involving association of a PMe_3 ligand or solvent. The observation that *trans*-**1** equilibrates with **2** in the presence of trace PMe_3 shows that a five-coordinate intermediate is accessible. If the concentration of **2** present in a solution of *cis*- and *trans*-**1** is small, the NMR resonances may not be noticeably broadened. A mechanism in which a solvent molecule coordinates to the platinum center may also operate. It is unlikely that solvent would displace a phosphine or hydride ligand, but pseudorotation of a five-coordinate solvato species is possible. An alternative uncatalyzed mechanism for thermal isomerization of **1** through a pseudotetrahedral intermediate has been discounted theoretically as energetically unfavored by 50-60 kcal/mol.[23-25] The isomerization of four-coordinate trialkyl(triphenylphosphine)gold(III) complexes, however, was postulated to occur through a tetrahedral transition state.[21]

An alternative dissociative mechanism suggested by a thoughtful reviewer is that the cis and trans isomers of **1** dissociate to different T-shaped isomers, which interconvert more slowly than they recoordinate PMe_3.

The faster rates for phosphine exchange from *cis*-**1**, as opposed to *trans*-**1** (Table II), suggest a dissociative exchange process. Phosphine in *cis*-**1** is labilized by trans hydride ligand, resulting in a faster rate of exchange with traces of the free ligand. This rapid exchange of phosphine ligands does not influence the rates of trans ↔ cis isomerization or reductive elimination of hydrogen from **1**. Phosphine exchange from *cis*-**1** at 25 °C occurs 10^6 faster than the rate of reductive elimination (Table II). Since the resonances for *cis*- and *trans*-**1** do not coalesce, the rate constant for isomerization at 25 °C is less than 300 s^{-1}, much slower than phosphine exchange (Table II). Thus, dissociation of PMe_3 cannot be the rate-limiting step in the isomerization. Since the Pt–H coupling constants for *cis*- and *trans*-**1** are not averaged by the phosphine exchange process, it is likely that the phosphine ligand dissociates to form a "T"-shaped species such as a or b. Formation of a "Y"-shaped species such as c would result in an average Pt–H coupling for each resonance.

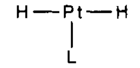

a

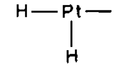

b

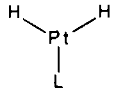

c

Reductive Elimination of Hydrogen. The observation of an inverse kinetic isotope effect for reductive elimination is significant. An inverse isotope effect is expected for the breaking of a low-frequency Pt–H bond and formation of a high-frequency H–H bond in the transition state.[56] This observation supports the predictions of the theoretical studies[23-25] of hydrogen reductive

---

(46) (a) Jones, W. D.; Feher, F. J. *J. Am. Chem. Soc.* **1985**, *107*, 620–631. (b) Jones, W. D.; Feher, F. J. *Ibid.* **1984**, *106*, 1650–1663. (c) Jones, W. D.; Feher, F. J. *Ibid.* **1986**, *108*, 4814–4819.

(47) (a) Janowicz, A. H.; Bergman, R. G. *J. Am. Chem. Soc.* **1983**, *105*, 3929–3939. (b) Bergman, R. G.; Seidler, P. F.; Wenzel, T. T. *Ibid.* **1985**, *107*, 4358–4359. (c) Wenzel, T. T.; Bergman, R. G. *Ibid.* **1986**, *108*, 4856–4857.

(48) Hackett, M.; Ibers, J. A.; Jernakoff, P.; Whitesides, G. M. *J. Am. Chem. Soc.* **1986**, *108*, 8094–8095.

(49) Lebrilla, C. B.; Maier, W. F. *J. Am. Chem. Soc.* **1986**, *108*, 1606–1616.

(50) (a) Basolo, F.; Pearson, R. G. *Mechanisms of Inorganic Reactions*, 2nd ed.; Wiley: New York, 1967. (b) Cooper, D. G.; Powell, J. *J. Am. Chem. Soc.* **1973**, *95*, 1102–1108. (c) Favez, R.; Roulet, R.; Pinkerton, A. A.; Schwarzenbach, D. *Inorg. Chem.* **1980**, *19*, 1356–1365. (d) Davies, J. A.; Uma, V. *J. Electroanal. Chem. Interfacial Electrochem.* **1983**, *158*, 13–24.

(51) (a) Redfield, D. A.; Cary, L. W.; Nelson, J. H. *Inorg. Chem.* **1975**, *14*, 50–59. (b) Redfield, D. A.; Nelson, J. H. *Ibid.* **1973**, *12*, 15–19. (c) Price, J. H.; Birk, J. P.; Wayland, B. B. *Ibid.* **1978**, *17*, 2245–2250.

(52) (a) Haake, P.; Pfeiffer, R. M. *J. Am. Chem. Soc.* **1970**, *92*, 4996–4997. (b) Louw, W. J. *Inorg. Chem.* **1977**, *16*, 2147–2160.

(53) Holt, M. S.; Nelson, J. H. *Inorg. Chem.* **1986**, *125*, 1316–1320.

(54) (a) Komiya, S.; Albright, T. A.; Hoffmann, R.; Kochi, J. K. *J. Am. Chem. Soc.* **1976**, *98*, 7255–7265. (b) Romeo, R.; Minniti, D.; Lanza, S. *Inorg. Chem.* **1980**, *19*, 3663–3668. (c) Romeo, R. *Ibid.* **1978**, *17*, 2040–2041.

(55) The equilibrium constants in THF and Me_2THF solvents were obtained by ^{31}P NMR spectroscopy at several temperatures between −80 and −40 °C and extrapolated to the temperature of this study. The equilibrium constant for Me_4THF was estimated from the ratio of the absorbances for *cis*- and *trans*-**1**, with the assumption that the ratios of IR extinction coefficients for *cis*- and *trans*-**1** are the same in Me_2THF and Me_4THF.

(56) Van Hook, W. A. In *Isotope Effects in Chemical Reactions*; Collins, C. J., Bowman, N. S., Eds.; Van Nostrand, Reinhold: New York, 1970.

Scheme I

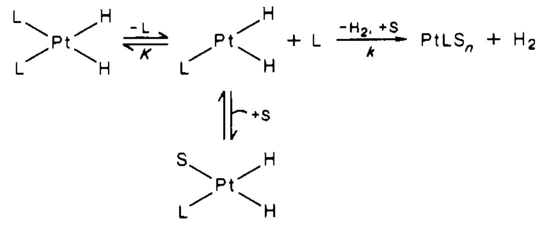

elimination, which conclude that the H–H bond forms nearly completely in the activated complex for reductive elimination. Alkane eliminations from metal centers also exhibit inverse isotope effects and have been interpreted in the context of a late transition state for elimination with appreciable C–H bond formation.[46c,47c] Our observed isotope effect might also be explained by reversible formation of an η^2-dihydrogen complex in a preequilibrium step (eq 6).[57] The equilibrium isotope effect favors an η^2-D_2 species over η^2-H_2, as its zero-point energy would be lower. In the oxidatively induced reductive elimination of hydrogen from $IrH_2(PEt_3)_2(nbd)^+$ in the presence of excess alkene (nbd = norbornadiene), the elimination of hydrogen was not observed directly, but was calculated to proceed with an inverse isotope effect attributed to a preequilibrium step.[58]

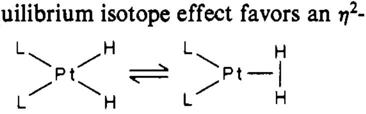

(6)

The expected kinetic isotope effect may be estimated for both possibilities.[57] Using the observed stretching frequencies for *cis*-PtH_2L_2, ν_{Pt-H} = 1980 cm^{-1} and ν_{H-H} = 4400 cm^{-1}, gives k_H/k_D = 0.51 for complete formation of an H–H bond in a late transition state, in good agreement with the observed value of 0.45. This isotope effect resembles that seen (0.51) recently[46] for a C–H reductive-elimination process in (η-C_5Me_5)Rh(H)(C_6H_5)(PMe_3). An inverse isotope effect of 0.7 was observed[15] for reductive elimination of cyclohexane from (η-C_5Me_5)Ir(H)(C_6H_{11})(PMe_3). For an η^2-H_2 species,[59] ν_{H-H} ~ 2550 cm^{-1} and yields a higher value of 0.85 for an isotope effect attributed to an η^2-H_2 intermediate formed in a preequilibrium step.

The dependence of the activation parameters for H_2 reductive elimination on the coordinating ability of solvent suggests an ordering of solvent molecules occurs as the reaction proceeds. Originally we attributed[6] this to collection of solvent molecules about a late transition state that resembles the reaction products, resulting in destabilization of the transition state (eq 7). However, this explanation may be inconsistent with transition state theory. If a reaction pathway having a lower $\Delta G^\ddagger$ is accessible in the absence of solvent coordination, that pathway should operate even in the presence of coordinating solvent unless solvent reorganization contributes significantly to $\Delta G^\ddagger$. Solvent coordination may also stabilize polar *cis*-**1** in the ground state and raise $\Delta G^\ddagger$, although this would not account for a large negative entropy of activation. A possible explanation involves large-scale reordering of the coordinating solvent (i.e. a solvent entropy effect) as the elimination proceeds.

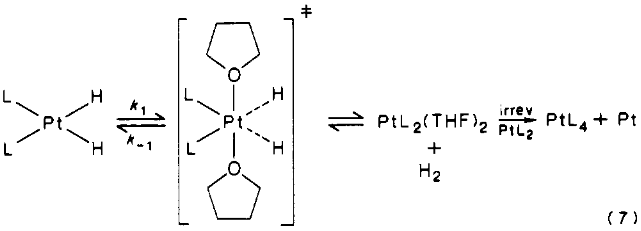

(7)

Table IV. Theoretical Predictions for H_2 Elimination from *cis*-PtH_2L_2

calcn	$\Delta H^\ddagger$, kcal/mol	ΔE, kcal/mol
	L = PH_3	
GVB[a]	18.2	+16.2
GVB-CI[b]	24.1	+6.7
RHF[c]	42.1	+36.9
SD-CI[c]	29.7	+21.5
	L = PMe_3	
SCF[b]	18.9	-0.6

[a] Reference 24. [b] Reference 23. [c] Reference 25.

Similar solvent effects were observed in the reductive elimination of ethane from bis(phosphine)dimethylpalladium(II),[18,19] with low activation enthalpies and large negative entropies found in coordinating solvents. Since added phosphine influenced the rate of reductive elimination, it was suggested phosphine dissociation, assisted by coordinating solvent, produced a three-coordinate $PdLMe_2$ species that underwent reductive elimination.[18,19] Because the phosphine ligands exchange rapidly (10^6 faster than reductive elimination) from *cis*-**1**, it is possible that reductive elimination of H_2 takes place from a 3-coordinate $PtLH_2$ species as in Scheme I. The three-coordinate complex may be "trapped" by a coordinating solvent molecule. Since elimination from a three- or five-coordinate complex occurs faster than elimination from a four-coordinate one,[8,60] solvent trapping would result in a slower rate of reductive elimination (Table III). It is important to note that *phosphine dissociation is not rate determining in either of the possible mechanisms*. The inverse isotope effect establishes Pt–H bond rupture as the rate-determining process. The rate of reductive elimination was not affected by the addition of a trace (1%) of PMe_3, but a detailed concentration study was not possible because of the associative reactivity with PMe_3 discussed earlier. It is possible that some free L produced in Scheme I assists H_2 reductive elimination from **1** before it is ultimately trapped as PtL_4.

The activation parameters determined for reductive elimination of H_2 from **1** may be compared with theoretical predictions for reductive elimination from the four-coordinate species. The complex $PtH_2(PH_3)_2$ has been studied by GVB,[24] GVB–CI,[23] RHF,[25] and SD–CI[25] methods. Calculated activation barriers and endothermicities for the reductive elimination are given in Table IV. The values of 18.1 and 24.1 kcal/mol approximate the value of 20.0 kcal/mol observed in noncoordinating 2,2,5,5-Me_4THF solvent. A SCF[23] calculation for *cis*-$PtH_2(PMe_3)_2$ yields an activation barrier of 18.9 kcal/mol for hydrogen reductive elimination. The calculated exothermicity of –0.6 kcal/mol agrees with the observation that solutions of **1** in 2,2,5,5-Me_4THF decompose readily on removal of H_2; i.e., $\Delta G \sim 0$. It is interesting that this calculation predicts disparate energies for *cis*- and *trans*-**1**, (ΔH_{isom} = 23 kcal/mol) in contrast to the negligible difference in their stability observed experimentally.[5] If the $\Delta H^\ddagger$ of 20.0 ± 0.5 kcal/mol is taken as the intrinsic barrier to reductive elimination of H_2, assuming $T\Delta S^\circ \sim 0$ in Me_4THF and $DH_m{}^\theta$ (H–H) = 104 kcal/mol, the Pt–H bond enthalpy may be esimated to have an upper limit of 62 kcal/mol. This agrees closely with theoretical estimates of 60 kcal/mol for the Pt–H bond dissociation energy[24,61] and with a tabulation[62] of available data on transition metal–hydride bond dissociation energies (most lie close to 60 kcal/mol).

Conclusion

This study emphasizes the mechanistic complexity of the "simple" dihydride complex $PtH_2(PMe_3)_2$, which undergoes structural isomerization, phosphine ligand exchange, and reductive elimination of hydrogen by independent kinetic processes. For

---

(57) Melander, L.; Saunders, W. H. *Reaction Rates of Isotopic Molecules*; Wiley: New York, 1980, p 27 log (k_H/k_D) = (0.081/T) ($w_{gs} - w^\ddagger$), where w_H/w_D = 1.35, w_{gs} = ground state frequency and $w^\ddagger$ = transition state frequency. This assumes a nonlinear transition state as considered for C–H reductive-elimination processes.[46c]

(58) Howarth, O. W.; McAteer, C. H.; Moore, P.; Morris, G. E. *J. Chem. Soc., Dalton Trans.* **1984**, 1171–1180.

(59) This value is an average of IR stretching frequencies for coordinated H_2 reported in ref 34–37.

(60) Tatsumi, K.; Hoffmann, R.; Yamamoto, A.; Stille, J. K. *Bull. Chem. Soc. Jpn.* **1981**, *54*, 1857–1867.

(61) Pearson, R. G. *Chem. Rev.* **1985**, *85*, 41–49.

(62) Halpern, J. *Inorg. Chim. Acta* **1985**, 100, 41–48. Skinner, H. A.; Connor, J. A.; *Pure Appl. Chem.* **1985**, *57*, 79–88.

the H_2 reductive-elimination process of importance to homogeneous and heterogeneous hydrogenation catalysis, the isotope effect observed supports the model of a late transition state where the H–H bond forms nearly completely either in the transition state or in a metastable η^2-H_2 intermediate. The relatively low (10–20 kcal/mole) enthalpies of activation for hydrogen reductive elimination for these late metal dihydrides emphasize the small energy difference between the dihydride, η^2-dihydrogen, and free dihydrogen structures. The high stability of platinum(II) dihydrides that contain bulky phosphine ligands must derive primarily from kinetic stability. Our results show that hydrogen reductive elimination is surprisingly solvent sensitive, with the dihydride complex being kinetically stabilized in polar-coordinating solvents. Invoking the principle of microscopic reversibility allows this solvent effect to be viewed in another context. Addition of molecular hydrogen to form a *cis*-dihydride complex must involve some charge separation, and polar solvents might aid in stabilizing dihydride formation.

The similarity between the isotope effects for dihydrogen reductive elimination, and those observed recently[15,46] for alkane elimination from late metal centers, suggests a similarity in the reverse processes of hydrogen and hydrocarbon activation. Crucial to the success of these reactions will be the proper η^2-orientation of the C–H or H–H bond so that the transition state for oxidative addition can be reached. Thus, aside from the thermodynamic constraints,[61,62] the kinetic limitations to C–H activation[15] may arise from steric barriers to achieving the η^2-precursor geometry. Indeed in late metal systems, where there is evidence for concerted C–H oxidative addition,[47] tertiary C–H groups in hydrocarbons show no reactivity.

Acknowledgment. This material is based on work supported by the National Science Foundation (Grant CHE-8504088). We thank Johnson Matthey for a sample of K_2PtCl_4 under their metal loan program. We thank Charles L. Perrin, Tammy Dwyer, and John Thoburn for assistance with spin-saturation-transfer experiments and with spectral simulations.

Registry No. $PtH_2(PMe_3)_2$, 103530-01-4; $PtH_2(PMe_3)_3$, 113705-04-7; Me_3P, 594-09-2; D_2, 7782-39-0.

Contribution from the School of Chemical Sciences,
University of Illinois at Urbana-Champaign, Urbana, Illinois 61801

Synthesis and Characterization of Coordinately Unsaturated Phosphine Complexes of Divalent V, Cr, Mn, Fe, and Co. Crystal Structures of $[CrCl_2(dippe)]_2$ and $FeCl_2(dippe)$

Ann R. Hermes and Gregory S. Girolami*

Received December 4, 1987

The reaction of divalent transition-metal halides with the bulky chelating phosphine 1,2-bis(diisopropylphosphino)ethane, dippe, gives a series of coordinately unsaturated complexes of stoichiometry MX_2(dippe) for M = V, Cr, Mn, Fe, or Co. Both the vanadium(II) and chromium(II) complexes readily form adducts with tetrahydrofuran or acetonitrile. The base-free chromium species exists as a dimer in the solid state, $[CrCl_2(dippe)]_2$, that consists of two square-planar chromium centers arranged in pairs via asymmetric chloride bridges. Averaged distances for the two independent molecules are as follows: Cr···Cr = 3.605 (2) Å; Cr–P = 2.481 (2), 2.511 (2) Å; Cr–Cl(t) = 2.333 (2) Å; Cr–Cl(b) = 2.380 (2), 2.606 (2) Å. Crystal data for $Cr_2Cl_4P_4C_{28}H_{64}$: space group $P\bar{1}$, $a = 13.225$ (2) Å, $b = 14.834$ (3) Å, $c = 11.101$ (2) Å, $\alpha = 97.35$ (1)°, $\beta = 114.21$ (1)°, $\gamma = 84.26$ (1)°, $V = 1967.3$ (6) Å^3, $Z = 2$, $R_F = 4.2\%$, $R_{wF} = 4.7\%$ on 3435 reflections and 344 variables. The manganese, iron, and cobalt complexes are all tetrahedral monomers, as confirmed by the X-ray crystal structure of $FeCl_2$(dippe): Fe–P = 2.46 (1) Å, Fe–Cl = 2.21 (1) Å, P–Fe–P = 83.8 (3)°, Cl–Fe–Cl = 117.1 (4)°. Crystal data for $FeCl_2P_2C_{14}H_{32}$: space group *Pbca*, $a = 24.66$ (1) Å, $b = 22.67$ (1) Å, $c = 14.995$ (6) Å, $V = 8385$ (8) Å^3, $Z = 16$, $R_F = 12.0\%$, $R_{wF} = 12.6\%$ on 1547 reflections and 201 variables. NMR and EPR studies show that all of the four-coordinate species exist in high-spin electronic configurations. The MX_2(dippe) complexes provide an excellent opportunity to examine the behavior of coordinately unsaturated first-row transition-metal species and serve as excellent starting materials for the preparation of low-electron-count organometallic derivatives of these elements.

Introduction

There are few areas of inorganic chemistry in which research activity is as great as the study of transition-metal complexes that contain phosphine ligands.[1,2] Organophosphines are able to stabilize metals in a wide variety of oxidation states and are unequaled as attendant ligands in many homogeneous catalytic processes.[3] The usefulness and versatility of phosphine ligands arise in part from their ability to engage in synergistic σ-donor and π-acceptor interactions with metal atoms and also from the chemist's ability to vary these electronic properties in a systematic fashion. The steric parameters of an organophosphine ligand can likewise be varied over a large range, essentially independently of its electronic properties.[4] Accordingly, the coordination number, coordination geometry, electron richness of a metal center, and the thermodynamics and kinetics of associative and dissociative equilibria can be tailored almost at will by a judicious choice of the substituents on phosphorus.

Our research is directed toward the preparation and study of coordinately unsaturated metal complexes, particularly of the early first-row transition elements.[5-13] Our approach is to employ phosphine ligands possessing appropriately selected electronic and steric properties that stabilize molecules in which the transition metal adopts an unusual electron count, coordination geometry, or oxidation state. Such species are expected to exhibit enhanced reactivity compared with that of coordinately saturated analogues.

The large atomic radii and the relatively electropositive nature of low-valent early transition elements suggest that electron-donating phosphines should best serve as ligating groups. Previous

---

(1) McAuliffe, C. A. *Transition Metal Complexes of Phosphorus, Arsenic, and Antimony Ligands*; Macmillan: New York, 1973.

(2) McAuliffe, C. A.; Levason, W. *Phosphine, Arsine and Stibine Complexes of the Transition Elements*; Elsevier: New York, 1979.

(3) Pignolet, L. H. *Homogeneous Catalysis with Metal Phosphine Complexes*; Plenum: New York, 1983.

(4) Tolman, C. A. *Chem. Rev.* **1977**, *77*, 313.

(5) Jensen, J. A.; Girolami, G. S. *J. Chem. Soc., Chem. Commun.* **1986**, 1160.

(6) Hermes, A. R.; Girolami, G. S. *Organometallics* **1987**, *6*, 763.

(7) Hermes, A. R.; Girolami, G. S. *Organometallics* **1988**, *7*, 394.

(8) Jensen, J. A.; Girolami, G. S. *J. Am. Chem. Soc.*, in press.

(9) Morris, R. J.; Girolami, G. S. *Organometallics* **1987**, *6*, 1815.

(10) Gardner, T. G.; Girolami, G. S. *Organometallics* **1987**, *6*, 2551.

(11) Gardner, T. G.; Girolami, G. S. *J. Chem. Soc., Chem. Commun.* **1987**, 1758.

(12) Hermes, A. R.; Morris, R. J.; Girolami, G. S., submitted for publication in *Organometallics*.

(13) Jensen, J. A.; Wilson, S. R.; Schultz, A. J.; Girolami, G. S. *J. Am. Chem. Soc.* **1987**, *109*, 8094.

0020-1669/88/1327-1775$01.50/0